METHODOLOGY FOR *IN SITU* CHARACTERISATION OF A HIGHLY BIREFRINGENT PHOTONIC CRYSTAL FIBRE FOR SUPERCONTINUUM GENERATION

J. P. Burger*, A. Ben Salem, R. Cherif** and M. Zghal****

** National Metrology Institute of South Africa (NMISA), Private Bag X34, Lynnwood Ridge, 0040, South Africa. E-mail: JBurger@nmisa.org*
*** Cirta'Com Laboratory, Engineering School of Communication of Tunis (Sup'Com), University of Carthage, Ghazala Technopark, Ariana 2083, Tunisia*

Abstract: A novel methodology for precisely determining the eigenaxes and effective twist of a solid-core polarisation maintaining fibre with a slightly elliptical effective core in an experimental setup with an ultrashort pulse laser is presented. This geometrical identification relies on experimental modal analysis and by utilising an incoherent ultrashort optical pulse fragment measurement and modelling procedure, and is a prerequisite for precise measurements and characterisation of this class of fibres. This orienting method is applied in the study of low threshold and temporally and polarisation stable supercontinuum generation in ~2m length of photonic crystal fibre, utilizing a modelocked Ti:Sapphire laser.

Key words: Polarisation maintaining fibre, orientation measurement, supercontinuum, photonics

1. INTRODUCTION

Polarisation-maintaining (PM) optical fibre has some physical provision for maintaining the state of linearly polarised light traveling through a single-mode core as is needed in various applications. Alignment and angular position determination of such fibre is important in the manufacturing, characterisation and utilisation of the fibre [1]. A number of methods are mentioned in literature for orienting such fibres. The first consists of applying a compressive stress to the side of a PM fibre and observing a change in the fibre's polarisation crosstalk or extinction ratio [2]. One can furthermore use imaging [3, 4] (which might utilise phase contrast) and some derivatives of this are used on modern fusion splicers. Side illumination with a laser and resultant scattering can also be used [5]. Other methods like monitoring the ellipticity of polarisation (see [6] and references therein) cannot discern between the fast and slow axis and are of more limited value. Much higher birefringence and stronger confinement are available in newer photonic crystal fibres (PCFs) [7] as compared to the traditional solid glass (PM) fibres. The latter attributes make PCFs attractive for a range of applications, including supercontinuum (SC) generation via nonlinear spectral broadening of ultrashort optical pulses [8-13]. Advantages of using birefringent PCF include the fact that all the spectral components exhibit the same stable linear polarisation and a reduced power requirement for SC generation [14]. Stable polarisation becomes important in especially optical frequency measurement and divider systems based on optical frequency combs [15]. Optical comb systems have been shown to be high precision frequency dividers for atomically stabilised optical oscillators (i.e. lasers) to generate high precision radio frequency (RF) clocking. Co-aligned and stable polarisation in the comb and the polarised laser (under test) are important in ensuring amplitude stability and low noise in the RF beat signal.

Despite all this previously mentioned work, there is to our knowledge, no published work, on the precise orientational measurement of PM-PCFs, as needed in characterisation and utilisation of such fibres. This is important especially when longer fibre strands are used, and twist is present in the fibre. The previously mentioned methods utilising imaging [3, 4] becomes hard at the high magnification needed for PCFs, and side illumination [5] becomes essentially impossible to decipher due to the large number of airholes, that can essentially block the view of the central area. The elasto-optic method [2] requires special piezoelectric contacts on the fibre, and it is not clear how stresses will propagate to the core of the PCF as opposed to solid glass fibres. Typically light is simply injected into the PCF using precision mechanical stages, and it is impossible to position high magnification microscopes in the same setup for viewing the fibre end-faces which have airholes of the order of ~100 to 500 nm in size. Therefore imaging for determining fibre orientation is impossible *in* the setup where the fibre is utilised, and moving the whole setup to a high magnification microscope is also difficult and would require special chucks for the fibre ends for mounting in a special microscope adapter.

A novel method for rapidly determining the orientation of a high birefringence PM-PCF in a setup where the fibre is simply put by hand into V-grooves is presented. This method would be especially applicable to the testing of these fibres in a manufacturing or research environment, where for example the nonlinearity also needs to be extracted. The method is based on modal analysis and measurement of the polarisation response with an ultrashort pulse probing laser. The abovementioned orientational information extracted by the new method and electromagnetic modelling was also utilised in the nonlinear optics study of the photonic crystal fibre that was investigated for generating octave

spanning supercontinua at *low* energy input (~100pJ) from a modelocked Ti:Sapphire laser. Such energy levels are now in the same energy range as those originating from high repetition rate fibre oscillators that are being developed [15-18] (of which nearly fully spliced versions could be made). These high repetition rate sources might offer *ab initio* measurement of precision optical frequency standards, without the need for a wavemeter due to the large longitudinal mode spacing. The type of fibre that was used in this study could potentially be used with such fibre sources, for stable low energy threshold SC.

2. EXPERIMENTAL SETUP

The experimental setup consisted of a modelocked linearly polarised Ti:Sapphire laser (it can run in continuous wave mode as well) that is coupled to a PM-PCF via a precision stage and a single objective lens. The laser produced ~56 fs (full width at half maximum) long pulses at 202 MHz repetition rate. The input polarisation into the fibre was controlled with a half-wave plate. At the output of the fibre the light was collimated with a lens and sent through an analyser (polariser). The output of the analyser could be sent to a wavelength insensitive power detector or optical spectrum analysers. The fibre mounting simply consisted of V-grooves in steel, with magnets pressing down on the fibre in the V-grooves. A fixed length of PM-PCF (2m) wound around a glass beaker was used in all the experiments.

3. MODAL MEASUREMENTS

2.1 Fibre analysis

Scanning electron microscopy (SEM) and finite element modelling was utilised in the present case on a commercial small core PCF with birefringence ~7×10^{-4} and a nonlinear coefficient of ~2.5×10^{-20} $m^2.W^{-1}$ to determine the theoretical modes. Most fibres are manufactured to have fully rotationally symmetric modes, but with highly nonlinear and high birefringence PM-PCF, as used here, it is possible to observe pronounced geometric elongation in the modes. The core of the fibre is shown in Figure 1, and it was determined that both polarisation modes are elongated along the slow axis, due to presence of two larger holes along the fast axis. Therefore measurements of the near and far-field were undertaken to determine the output axes in the setup.

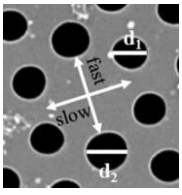

Figure 1: A SEM micrograph of the core region of the PM-PCF. The distance between the two large airholes centre is approximately 2 µm.

2.2 Near-field measurement

The near-field was imaged with a high numerical aperture (NA) aspheric lens onto a charge coupled device focal plane array (CCD) as shown in Figure 2. Such a near-field image (screen capture) is shown in Figure 3, together with measured cross-sections and is rotated by 90 degrees (for the correct view), to compensate for the 90 degree mounting of the array in the laboratory. From the image it can already be seen that the fast axis is nearly perpendicular with the optical table's surface, because of the horizontal elongation of the beam. The determination of axes was done by calculating second order moments (σ^2_x and σ^2_y) along straight lines going through the numerical mass centres of the images, when the images were rotated (Figure 4). The *x*-axis is parallel to the laboratory optical table and the *y*-axis perpendicular. An analysis of Figure 4 indicated the angle of the fast axis to be -1°. The near-field image is very sensitive to focusing and therefore the far-field was also examined to check the correctness of this measurement.

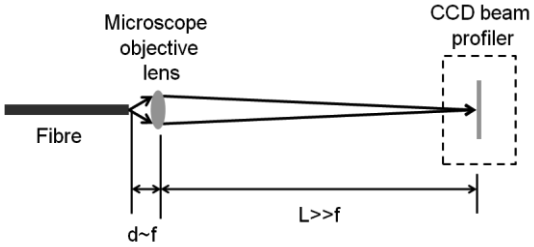

Figure 2: The experimental setup utilised for measuring the near-field. The microscope objective is placed at a distance d nearly equal to the focal length f from the fibre; and a much enlarged image is formed at a distance L>>f onto a focal plane array.

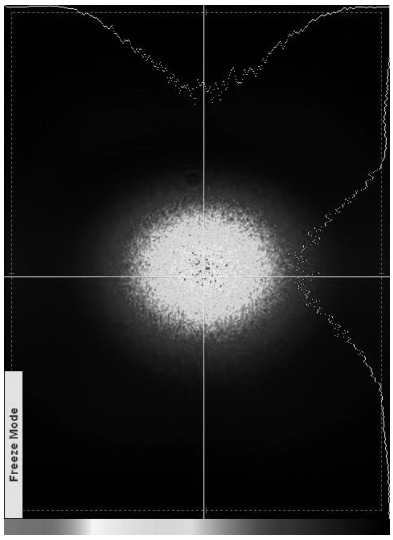

Figure 3: Near-field image of the fibre mode.

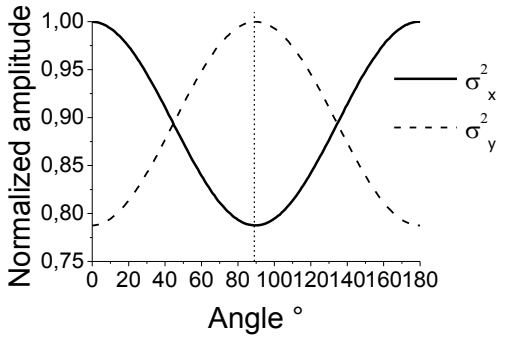

Figure 4: Second moments of the image in Figure 3.

2.2 Far-field measurement

The far-field was projected onto a diffusing screen in the focal point of a large high NA lens, when the lens is less than a focal length away from the fibre as shown in Figure 5. A CCD camera was then used to take an image of the diffusing screen (Figure 6) and the second moments calculated (Figure 7). The results indicated that the major axis of the image was at 89º.

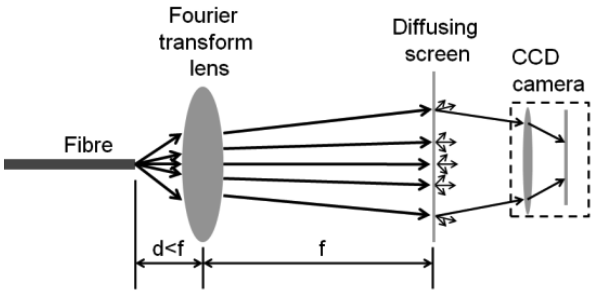

Figure 5: Setup utilised for far-field measurement. f is the focal length of the Fourier transform lens.

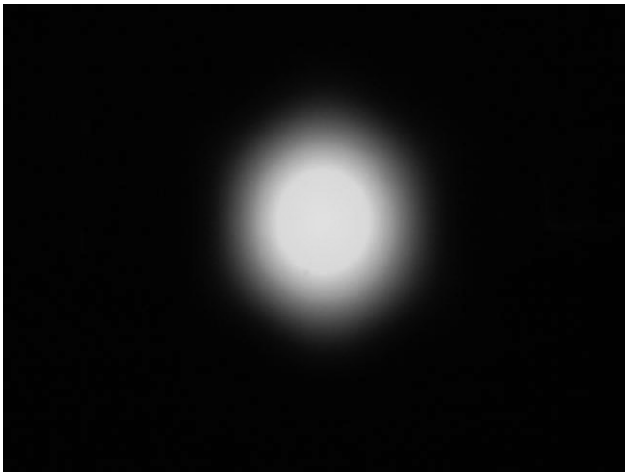

Figure 6: Image of the far-field.

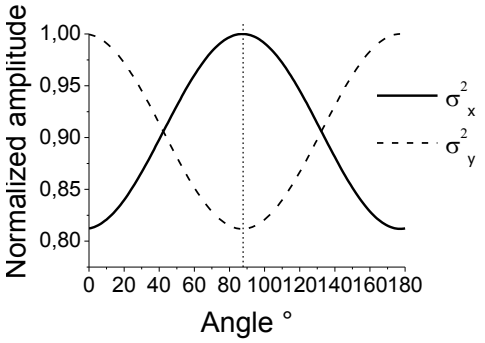

Figure 7: Second moments of the far-field.

2.3 Discussion

The far-field orientation was determined to be exactly as expected; it exhibited a a 90º degree rotational difference w.r.t. the near-field, and therefore the near and far-field measurements are consistent in showing a -1º orientation of the fast axis at the fibre output. The input side of the fibre still had an unknown orientation, which could be determined through polarisation measurements as shown in the next section.

4. POLARISATION RESPONSE WITH ULTRASHORT PULSE INJECTION

4.1 Model

The fibre is probed with ultrashort pulses and it was shown by ultrashort pulse propagation modelling [13] that the polarisation mode dispersion was such that two temporally separated orthogonally polarised pulse fragments were created in the first few cm of the fibre. Under such circumstances the pulse fragments were incoherent at the output of the fibre. Nonetheless, a Jones matrix analysis of the system can be undertaken, if new Jones projection matrices are introduced [20]. This analysis predicts an output intensity dependence on polarisation (polarisation response) as follows:

$$
\begin{aligned}
I_{out} \propto\ & \cos^2(\Psi)\cos^2(\Psi-\varepsilon)\times \\
& \left\{\begin{array}{l}
\cos^2(\kappa)\sin^2(\kappa) \\
-2\sin(\zeta)\cos(\zeta)\times\left[\cos^3(\kappa)\sin(\kappa)+\cos(\kappa)\sin^3(\kappa)\right]+ \\
\cos^2(\zeta)\cos^4(\kappa)+\sin^2(\zeta)\cos^4(\kappa)
\end{array}\right\} \\
+\quad & \sin^2(\Psi)\sin^2(\Psi-\varepsilon)\times \\
& \left\{\begin{array}{l}
\cos^2(\kappa)\sin^2(\kappa) \\
-2\sin(\zeta)\cos(\zeta)\times\left[\cos^3(\kappa)\sin(\kappa)+\cos(\kappa)\sin^3(\kappa)\right]+ \\
\sin^2(\zeta)\cos^4(\kappa)+\cos^2(\zeta)\cos^4(\kappa)
\end{array}\right\}
\end{aligned}
\tag{1}
$$

The angular symbols are defined in Table 1.

Table 1: Definition of angles.

Angle symbol	Definition
ψ	Input polarisation angle
ε	Angle of fast axis of the PCF at the input side of the PCF.
η	Angle of fast axis of the PCF at the output side of the PCF.
ζ	Twist angle in order to give the fast axis orientation at the input side of the PCF ($\zeta=\eta-\varepsilon$).
κ	Angle of the polarisation axis of the polarizer

In order to demonstrate the sensitivity of the output response to the fibre rotation, two polarisation response surfaces are calculated for firstly ε = 5º and η = 6º (Figure 8) and then ε = 5º and η = 8º (Figure 9), i.e., only a 2º difference in output angle/twist. The clear sensitivity of the response to the system angles makes the intensity dependence on the polarisation ideal for determining the fibre twist.

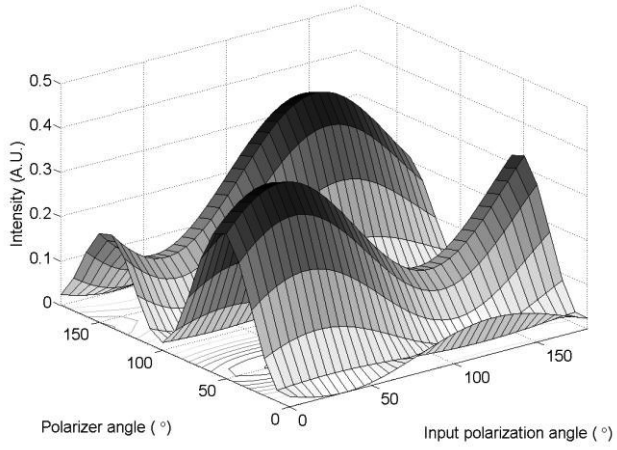

Figure 8: Theoretical polarisation response for ε = 5º and η = 6º.

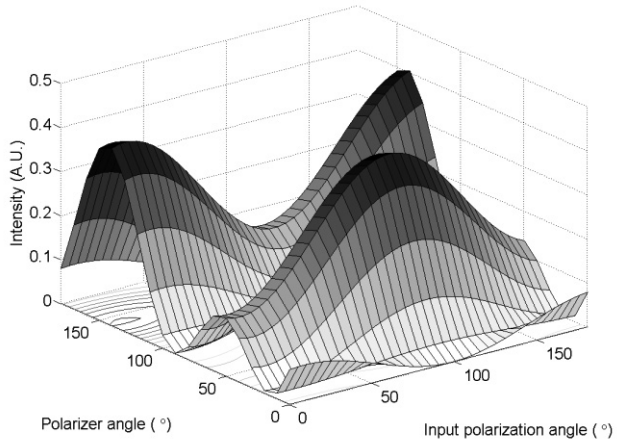

Figure 9: Theoretical polarisation response for ε = 5º and η = 8º.

4.2 Measurements

The polarisation response methodology was applied to the fibre utilised in the study. A measurement of the polarisation response is shown in Figure 10. The graph was surface-fitted as a function of fibre twist to yield a single solution: a fibre twist angle of 85.2º. The theoretical response is shown in Figure 11.

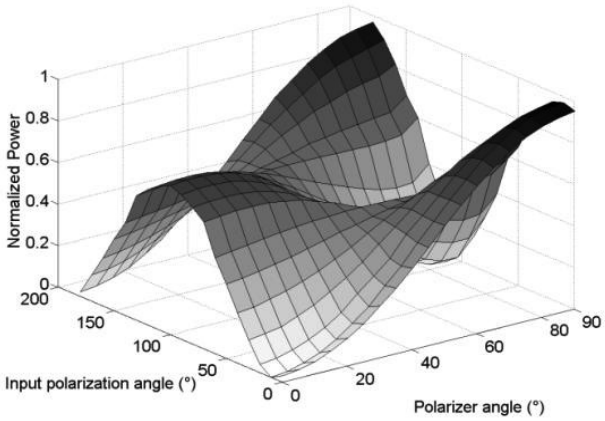

Figure 10: Experimental polarisation response.

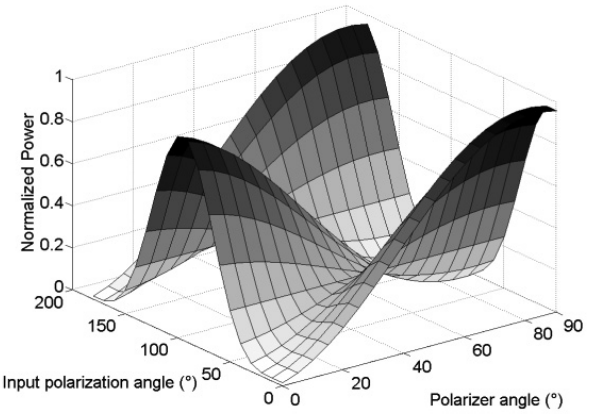

Figure 11: Theoretical polarisation response.

4.3 Discussion

The shapes shown in Figures 10 and 11 are very similar and smaller, unmodelled effects are responsible for some differences. Firstly, the model assumes perfect polarisation extinction is possible in the fibre. The fibre exhibited an imperfect polarisation extinction of ~ -15 dB and the underlying mechanisms implied by this could possibly explain discrepancies. The unaccounted-for mechanisms include the fact that launching with a strongly focused beam implies deviation from the linear polarisation input [21]. Furthermore eigenmodes are in fact hybrid [22], and even more so in strongly guided structures such as the fibre used here. Furthermore, birefringent fibres are known to have coupling between polarisation modes due to inevitable non-uniformity along the length of fibre [22]. Lastly the laser beam from

the modelocked laser is slightly elliptical with some substructure, and this geometric structure is also expected to play a role in the polarisation at the focus where the fibre is situated.

5. APPLICATION IN SC STUDIES

Polarisation resolved studies were also undertaken on the same fibre after the axes were determined. Pulses with energy of ~100 pJ per pulse were injected into the fibre. Spectra were recorded as a function of input and output polarisation (for steps of 5º degree rotation) and some of these are shown in Figures 12-14 with the angles referenced with respect to the fast axis at the input. The spectra as shown are contour maps of the logarithm of spectral density. White signifies the highest intensity. The slight smearing coupled with blotchiness is because of the relatively coarse 5º sampling interval and interpolation that MATLAB's contour plot algorithm utilizes. The main features of the SC can be clearly seen though. The nature of supercontinuum generation is complex [8], and in-depth discussions are beyond the scope of this paper. The main features can be easily recognized from the graphs that are shown here.

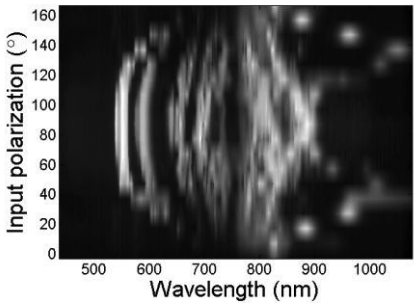

Figure 12: Output spectra recorded on fast axis.

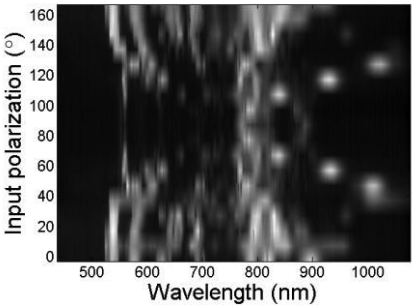

Figure 13: Output spectra recorded on slow axis.

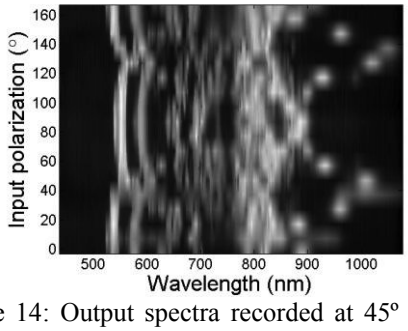

Figure 14: Output spectra recorded at 45º w.r.t. the fast axis.

Figure 12 shows the spectral evolution as a function of injected power - starting from zero power (at input polarisation of 0º). The laser spectrum is initially centred at 820 nm, and the measurement at 0º input polarisation is mostly polarisation leakage, with little nonlinear signature. A series of dots starts forming to the right as the input polarisation angle is increased (this should be a streak, but is not finely sampled enough here). These dots represent a redshifted Raman soliton (others can also just be seen forming at higher power corresponding to close to 90º polarisation). The fibre initially supports an *N*-th order soliton for the first section [10], if one assumes that all the light is falling above the zero-dispersion wavelength. Because of higher order dispersion and nonlinear effects, this higher order soliton decays into redshifted fundamental solitons along with blue shifted nonsolitonic radiation. The curved waves on the right hand side of Figure 12 are literally the spectral signatures of the dispersive waves (blue shifted nonsolitonic radiation), and the blue shift is clearly power dependent. Some radiation was recorded up to 1400 nm (not shown here), and more than an octave of bandwidth is spanned, even though the spectrum was not flat. The spectra were very stable on timescales exceeding a month. Figure 13 is essentially the same as Figure 12, except that the whole image is effectively 90º phase shifted. This represents the spectra along the slow axis, for a range of input powers (the lowest input power would correspond to 90º input polarisation). Figure 14's measurement essentially shows a mixture of Figure 12 and 13 as it represents the radiation at 45º w.r.t. both the slow and fast axis. In the experiment leading to Figure 14 half of the radiation in Figure 12 and Figure 13 are detected simultaneously. Interestingly, a larger blue shift is seen for one of the polarisation's dispersive waves than the other's and could be attributable to the fact that zero-dispersion wavelength for the two polarizations are predicted to be 15 nm apart, and close or even inside the pump spectrum, leading to different degrees of soliton-effect compression of the pump pulse for the two polarizations.

6. CONCLUSION

A novel method for measuring the orientation of PM-PCF at both the input and output ends have been presented. The method requires the fibre to be simply mounted in V-grooves by hand and furthermore needs only a CCD imager, power meter, inexpensive lenses and a waveplate and polarizer. A short pulse modelocked Ti:Sapphire laser was utilised in the measurement. It would also be straightforward to also measure the birefringence in the same setup, by measuring the separation of two pulse fragments (at lower energy than shown here to avoid most fibre nonlinearities) with a second-harmonic autocorrelator [23] (usually available in an ultrafast optics laboratory). Small discrepancies were measured between the theoretical and modelled polarisation response, and was discussed. The latter discussion illustrates that there is further scope, to study smaller polarisation effects in PM-PCF, which could be significant in some niche

applications. SC studies were also undertaken on the same fibre as used in the orientation measurement. The measurements showed greater than an octave of bandwidth of SC by using less than 100 pJ of input energy and a relatively long length of fibre. The spectra were also very stable in time, possibly making this class of fibre useful for use in optical combs based on high repetition rate modelocked fibre lasers, if high coherence could also be demonstrated.

7. ACKNOWLEDGEMENTS

Funding was obtained the African Laser Centre and the research initiative at the NMISA for this work. Clive Oliphant is thanked for SEM micrographs, and Sara Prins and Ronnie Kritzinger for proofreading.

8. REFERENCES

[1] J. Noda, K. Okamoto and Y. Sasaki: "Polarization Maintaining Fibers and Their Applications", *Journal of Lightwave Technology*, Vol. 4, No. 8, pp. 1071-1089, August 1986.

[2] S. L. A. Carrara, B.Y. Kim and H. J. Shaw: "Elasto-optic alignment of birefringent axes in polarization-holding optical fiber", *Optics Letters*, Vol. 11, No.7, pp. 470-472, July 1986.

[3] Fujikura Ltd. product bulletin #88112000 on the FSM-20 PM, p. 2, 1990.

[4] Y. Hu, J. Tan, Z. Chen, C. Zeng, S. Chang and Z. Meng: "Phase contrast method for measurement of birefringent axes orientation of polarization-maintaining fiber", *Proceedings of the International Society for Optical Engineering*, Vol. 2895, pp. 350-354, 1996.

[5] J. B. Aniano: "System for determining birefringent axes in polarization-maintaining fiber", *U.S. Patent 5317575*, May 1994

[6] D. de Oliveira Maionchi, W. Campos and J. Frejlich: "Angular alignment of a polarization-maintaining optical fiber", *Optical Engineering*, Vol. 40, No. 7, pp. 1260-1264, July 2001.

[7] K. Suzuki, H. Kubota, S. Kawanishi, M. Tanaka and M. Fujita: "Optical properties of a low-loss polarization-maintaining photonic crystal fiber", *Optics Express*, Vol. 9, No. 13, pp. 676-680, December 2001.

[8] J. Dudley, G. Genty and S. Coen: "Supercontinuum generation in photonic crystal fiber", *Reviews of Modern Physics*, Vol. 78, pp. 1135-1184, October-December 2006.

[9] M. Lehtonen, G. Genty, and H. Ludvigsen and M. Kaivola: "Supercontinuum generation in a highly birefringent microstructured fiber", *Applied Physics Letters*, Vol. 82, No. 14, pp. 2197-2199, April 2003.

[10] A.Proulx, J-M.Ménard, N.Hô, J.M. Laniel, R.Vallée and C. Paré : "Intensity and polarisation dependences of the supercontinuum generation in birefringent and highly nonlinear microstructured fibers", *Optics Expres*s, Vol. 11, No. 25, pp. 3338-3345, December 2003.

[11] Z. Zhu and T. G. Brown: "Polarization properties of supercontinuum spectra generated in birefringent photonic crystal fibers," *Journal of the Optical Society of America B*, Vol. 21, No. 2, pp. 249-257, February 2004.

[12] Z.Zhu and T.G. Brown: "Experimental studies of polarization properties of supercontinua generated in a birefringent photonic crystal fiber", *Optics Express*, Vol. 12, No. 5, pp. 791-796, March 2004.

[13] A. Ben Salem, R. Cherif, M. Zghal, and J. Burger: "Highly Birefringent Photonic Crystal Fiber for Coherent Infrared Supercontinuum Generation", *Proceedings: Progress in Electromagnetics Research Symposium*, Marrakesh, Morocco, pp. 1247-1251, March 2011.

[14] P. Blandin, F. Druon, M. Hanna, S. L. Fort, C. Lesvigne, V. Couderc, P. Leproux, A. Tonello and P. Georges: "Picosecond polarized supercontinuum generation controlled by intermodal four-wave mixing for fluorescence lifetime imaging microscopy," *Optics Express*, Vol. 16, No. 23, pp. 18844-18849, November 2008.

[15] J. Ye and S.T. Cundiff (eds), *Femtosecond Optical Frequency Comb Technology: Principle, Operation and Applications*, Springer Science and Business Media, New York, 2005.

[16] S.Zhou, D.G. Ouzonov and F.M. Wise: "Passive harmonic mode-locking of a soliton Yb fiber laser at repetition rates to 1.5 GHz", *Optics Letters*, Vol. 31, No. 8, pp. 1041-1042, April 2006.

[17] J. Chen, J. W. Sickler, E. P. Ippen, and F. X. Kärtner: "High Repetition Rate, Low Jitter, Fundamentally Mode-Locked Soliton Er-Fiber Laser," *Conference paper: Conference on Lasers and Electro-Optics/Quantum Electronics and Laser Science Conference and Photonic Applications Systems Technologies*, OSA Technical Digest Series (CD) (Optical Society of America), paper CThHH3, May 2007.

[18] H. Byun, D. Pudo, J. Chen, E.P. Ippen, and F. X. Kärtner: "High-repetition-rate, 491 MHz, femtosecond fiber laser with low timing jitter", *Optics Letters*, Vol. 33, No. 19, pp. 2221-2223, October 2008.

[19] A. Martinez and S. Yamashita: "Multi-gigahertz repetition rate passively modelocked fiber lasers using carbon nanotubes", *Optics Express*, Vol. 19, No. 7, pp. 6155-6163 , March 2011.

[20] A. Ben Salem, Rim Cherif, M.Zghal and J.P.Burger: "Insights into the polarisation behaviour of a long birefringent photonic crystal fibre under low energy ultrashort pulse excitation", *Proceedings: 2011 IEEE Africon Conference*, Livingstone, Zambia, September 2011.

[21] J.Lekner: "Polarisation of tightly focused laser beams", *Journal of Optics A: Pure and Applied Optics* ,Vol. 5, No. 1, pp. 6–14, January 2003.

[22] T. A. Eftimov and W. J. Bock: "Analysis of the Polarisation Behavior of Hybrid Modes in Highly Birefringent Fibers", *Journal of Lightwave Technology*, Vol. 16, No. 6, pp. 998-1005, June 1998.

[23] J.P.Burger, W.H. Steier and S. Dubovitsky: " The energy-limiting characteristics of a polarisation-maintaining Sagnac interferometer with an intraloop compressively strained quantum-well saturable absorber", *Journal of Lightwave Technology*, Vol.20, No. 8, pp. 1382–1387, August 2002.